On the interlayer toughening of carbon fibre/epoxy composites using surface-activated ultra-thin PEEK films

Quan, Dong; Wang, Guilong; Zhao, Guoqun; Alderliesten, René

DOI
10.1016/j.compstruct.2022.116309

Publication date
2023

Document Version
Final published version

Published in
Composite Structures

Composite Structures 303 (2023) 116309

Contents lists available at ScienceDirect

Composite Structures

journal homepage: www.elsevier.com/locate/compstruct

On the interlayer toughening of carbon fibre/epoxy composites using surface-activated ultra-thin PEEK films

Dong Quan [a,b], Guilong Wang [a], Guoqun Zhao [a,*], René Alderliesten [b,*]

[a] Key Laboratory for Liquid–Solid Structural Evolution and Processing of Materials (Ministry of Education), Shandong University, China
[b] Structural Integrity & Composites Group, Faculty of Aerospace Engineering, Delft University of Technology, Netherlands

ARTICLE INFO

Keywords:
Polymer-matrix composites (PMCs)
Ultra-thin films
Interlayer toughening
Fracture toughness

ABSTRACT

The exceptional mechanical properties of Polyether-ether-ketone(PEEK) polymers make them ideal candidates for interlayer toughening of carbon fibre/epoxy composites. Herein, ultra-thin PEEK films with a thickness of 8 μm, 18 μm and 25 μm were used for interlayer toughening of an aerospace-grade carbon fibre/epoxy composite. The mode-I and mode-II fracture behaviour of the interleaved laminates were investigated, with the fracture mechanisms being investigated. The surfaces of the PEEK films were treated by a UV-irradiation technique to enhance their intrinsically low surface activities. This significantly increased the adhesion at the interface between the PEEK interlayers and the composite matrix. A topography analysis on the fracture surfaces revealed extensive damage of the PEEK interlayers during the fracture process of the laminates. Owing to the exceptional properties of the PEEK films, significant enhancements in the mode-I and mode-II fracture properties of the laminates were obtained, i.e. the mode-I and mode-II fracture energies were significantly increased by 227% and 441%, respectively. Overall, the UV-treated PEEK films proved superior effectivenesses for laminate toughening when compared to the other state-of-the-art interlayer materials.

1. Introduction

Carbon fibre/epoxy composites are widely used as load-bearing structures in multiple industries, including the aerospace, automotive and marine sectors. For example, the new generation passenger aircrafts, Boeing 787 and Airbus 350 contain over 50% of composite structures by weight, including the fuselage, wing and fan cowl door sections. Therefore, it is critical to assure the structural integrity of the composites during their terms of service. However, carbon fibre/epoxy composites are prone to interlaminar delamination, that can lead to considerable drops in their mechanical properties. This is attributed to the intrinsic low fracture toughness of the epoxy matrix and the laminated structure of the composites. Various techniques had been developed to enhance the interlaminar properties of carbon fibre/epoxy composites, with interlayer toughening [1], Z-pinning [2] and three-dimensional (3D) weaving [3] representing the most prevalent methods. Interlayer toughening offers many advantages over Z-pining and 3D weaving, including a high flexibility of interlayer selection, a possibility to add low cost to the laminate manufacturing and a potential to retain the in-plane mechanical properties of the laminates. A wide range of materials had been used as interlayer materials, including thermosetting films [4], carbon nanomaterials [5], metal fibres [6] and various thermoplastic phases [7,8]. Overall, significantly different levels of toughness improvements have been obtained by interleaving various materials into the laminates, and the areal density, form, and type of the interlayer materials, the architecture of the carbon fibres and the curing process of the laminates all played critical roles.

Thermoplastic materials are attractive candidates for the interlayer toughening of laminates, e.g. the previous work [9,10] showed that interleaving thermoplastic veils into the laminates simultaneously increased G_{IC} and G_{IIC} by over 200%. Thermoplastic interlayers can be added into the laminates in a shape of powder, film, scrim and non-woven fabric for interlayer toughening [8,11]. Among them, thermoplastic nanofibres had proved excellent toughening performance [12–14], and hence are currently most widely used. Additionally, depending on the types of thermoplastics and the curing process of the laminates, thermoplastics can be in different states in the cured laminates, i.e. being intact [15], partially or completely dissolved in the epoxy matrix [16] or molten during the laminate curing process [10]. All these possibilities offer a feasibility of using thermoplastic interlayers to tailor the mechanical, fracture and thermal properties of the laminates, and hence to satisfy the requirements of different applications.

* Corresponding authors.
E-mail addresses: zhaogq@sdu.edu.cn (G. Zhao), R.C.Alderliesten@tudelft.nl (R. Alderliesten).

https://doi.org/10.1016/j.compstruct.2022.116309
Received 7 May 2022; Received in revised form 11 August 2022; Accepted 6 October 2022
Available online 10 October 2022

Thermoplastic films are one of the most prevalent interlayers for laminate toughening, with a good toughening performance being reported in many studies [17–21]. For example, Yasaee et al. [17,18] used Polyimide (PI) thermoplastic film strips (50 μm in thickness) for interlayer toughening of a laminate, and observed an increase of 79% and 118% for the mode-I fracture energy (G_{IC}) and the mode-II fracture energy (G_{IIC}), respectively. Yao et al. [19] reported an improvement of 90.65% in G_{IC} by interleaving a layer of Polyetherketone-cardo (PEK-C) film (10 μm in thickness) into a laminate. Guo and Liu [20] demonstrated that interleaving structured PEK-C films into a laminate slightly increased G_{IC} by 17%, and significantly increased G_{IIC} by 325%. In another study, Mathew et al. [21] observed an obvious increase of 76% in G_{IC} of a laminate due to interleaving ethylene-vinyl acetate copolymer (EVA) film (220 μm in thickness). However, it also caused a considerable decrease of 55.4% in G_{IIC}. Similarly, Marino and Czel [22] reported that the addition of acrylonitrile-butadienestyrene (ABS) films (with a thickness of 30 μm and 60 μm) failed to improve the mode-II fracture toughness of a laminate. The poor toughening performance of the EVA and ABS films for the mode-II fracture was attributed to their poor mechanical properties under shear loading conditions [21,22]. Hence, the use of thermoplastic films with good mechanical properties is necessary for advanced laminate toughening. Additionally, a good adhesion/miscibility between the thermoplastic films and the epoxy matrix is also critical to achieve good mode-I and mode-II toughening performance [17–20].

Polyether-ether-ketone (PEEK) polymers possess exceptional mechanical properties and fracture toughness, and hence they are ideal candidates as interlayers of carbon fibre/epoxy composites. However, the number of studies using PEEK polymers for interlayer toughening of laminates is very limited. Quan et al. [23] studied the effects of interleaving continuous PEEK fibres on the fracture toughness and damage resistance of two aerospace-grade carbon fibre/epoxy laminates. It was reported that adding PEEK fibres significantly increased G_{IC} of an unidirectional (UD) laminate and a 5-harness weave (5H) laminate by 293% and 79%, respectively. Moreover, it had improved the Charpy impact strength and failure load of the open-hole tensile specimens of the 5H laminate by 131% and 29%, respectively. In another study, nowoven mats based on micro-size PEEK fibres were used by Ramirez et al. [24] for interlayer toughening of a laminate. An increase of about 100% and 380% was observed for G_{IC} and G_{IIC}, respectively due to interleaving the PEEK veils with an areal density of 11 g/m^2. These studies have clearly proven a high efficiency of PEEK polymers for interlayer toughening of composite laminates. However, only PEEK fibres were considered in these studies and the main toughening mechanism was observed to be PEEK fibre bridging during the fracture process of the laminates. Accordingly, no obvious damage and plastic deformation to the PEEK fibres were triggered during the fracture process [23,24], as a relatively poor PEEK/epoxy adhesion is required to obtain a high level of fibre bridging mechanism [25,26]. In this case, the excellent mechanical properties and fracture toughness of PEEK were not fully utilised. Moreover, a relatively poor PEEK/epoxy adhesion can cause negative effects to the hygrothermal resistance of the laminates. The foremost challenge to achieve good adhesion at the PEEK/epoxy interface lays with effectively improving the intrinsically low surface energies of the PEEK interlayers. This is especially critical for PEEK interlayers that typically possess micro/nano-scale dimensions, since traditional surface treatment techniques can cause obvious damage or thermal/chemical degradation to them. Encouragingly, our previous studies [25,27] demonstrated that the adhesion at the PEEK/epoxy and PPS/epoxy interface can be enhanced by applying a UV-treatment to the thermoplastic surfaces, without causing obvious damage to the micro-scale thermoplastic fibres. This allowed us to further explore the potential of utilising the outstanding mechanical properties of the PEEK polymers for laminate toughening in this study.

Herein, PEEK films with an ultra-thin thickness of 8 μm, 18 μm and 25 μm were selected as the interlayers for laminate toughening. From one aspect, the small thickness of the film interlayers can avoid significant drops in the volume fractions of the carbon fibres of the laminates, and largely retain the in-plane mechanical properties. From another aspect, to the best knowledge of the authors, there is still no research on the use of PEEK films for laminate interlayer toughening. The adhesion between the PEEK films and the epoxy matrix was tailored by applying a UV-treatment to the PEEK films for different durations. The PEEK films were then placed at the mid-plane of an aerospace-grade carbon fibre/epoxy composite for interlayer toughening. A systematic experimental study was carried out to investigate the effects of the PEEK film thickness and the PEEK/epoxy adhesion on the mode-I and mode-II fracture behaviour and toughening mechanisms of the interleaved laminates.

2. Experimental

2.1. Materials and sample preparation

The carbon fibre/epoxy prepreg was unidirectional HexPly IM7-8552 with a fibre volume fraction of 65% and an areal density of 134 g/m^2 from Hexcel, Germany. Thin PEEK films with a thickness of 8 μm, 18 μm and 25 μm were APTIV 1000 films supplied by Victrex, UK.

The surfaces of the PEEK films were UV-treated to improve their adhesion with the epoxy matrix of the laminate. The films were cleaned with iso-propanol carefully and then placed in an enclosed chamber (550 mm×170 mm×60 mm) that is equipped with three 30 W tube UVC-lamps for a UV-treatment. Different durations of treatments were carried out to both sides of the PEEK films. A unidirectional layup consisting of 40 plies of carbon fibre prepregs and one layer of UV-treated PEEK film at the mid-plane was prepared with a hand lay-up process, as schematically shown in Fig. 1 (a). This was done immediately after the UV-treatment process to avoid any contamination of the UV-treated PEEK surfaces. During the layup preparation process, a 10 min of de-bulking at an under pressure lower than 100 mbar was applied between every fourth layer. A piece of PTFE film with a thickness of 12.7 μm was also placed at the mid-plane to create crack starters within the fracture specimens. The layup was sealed in a vacuum bag on an Aluminium plate and then placed in a Scholz autoclave for curing. The curing schedule was 180 °C and 6 bar gauge pressure for 90 mins, during which a vacuum pressure of 200 mbar was kept inside the vacuum bag. A panel of reference laminate without PEEK interlayers was also prepared using the same manufacturing process. After the curing, the laminate panels were cut into desired dimensions for a double cantilever beam (DCB) test and an end-notched flexure (ENF) test, as schematically shown in Fig. 1 (b). Fig. 2 shows the side-view images of the laminates with PEEK interlayers. The yellow colour double head arrows indicate the interlayers. The thicknesses of the PEEK interlayers within the cured laminates were measured to be essentially identical to the given thicknesses of the PEEK films by the supplier. In Fig. 2 and the rest of this paper, the PEEK films were referred to as PEEK followed by the values of the thickness and then the duration of the UV-treatment in a bracket, i.e. PEEK8 means the PEEK films with a thickness of 8 μm, PEEK8(6UV) denotes the PEEK8 films were UV-treated for 6 mins and PEEK(6UV) represents all the PEEK films that were UV treated for 6 mins.

To study the effects of the UV-treatment on the adhesion at the PEEK/laminate interface, T-joint specimens were produced by co-cure joining a piece of PEEK bar onto the laminate. The setup for preparing the T-joints is schematically shown in Fig. 3 (a). A layup consisting of 20 plies of carbon fibre/epoxy prepregs was prepared by a hand layup process, with a 10 min of de-bulking at an under pressure lower than 100 mbar being applied between every fourth layer. A piece of PEEK bar (the same grade of PEEK from the same supplier) with a dimension of 100 mm×70 mm×2 mm was then assembled onto the prepreg, see Fig. 3 (a). Prior to that, the joining surface of the PEEK bar was grounded using 800 grit sandpapers and then UV-treated for

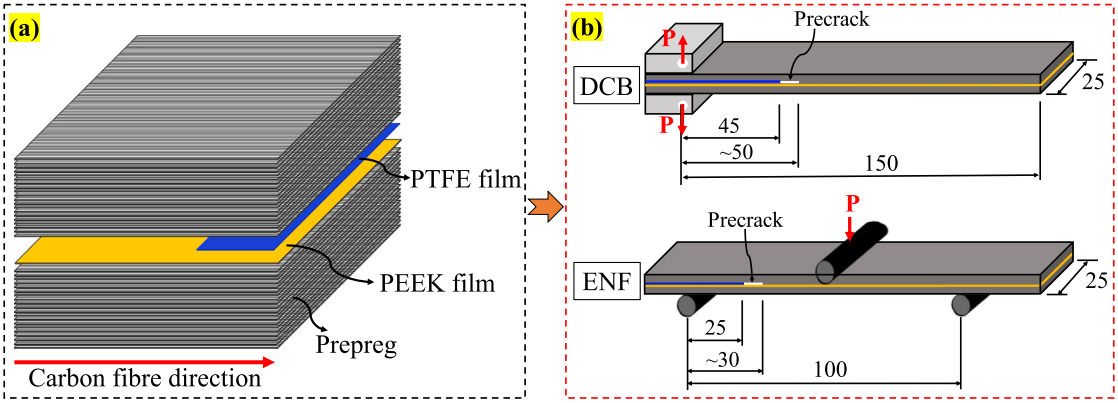

Fig. 1. Schematics of the (a) layups and (b) DCB and ENF specimens of the interleaved laminates. The units in (b) are mm.

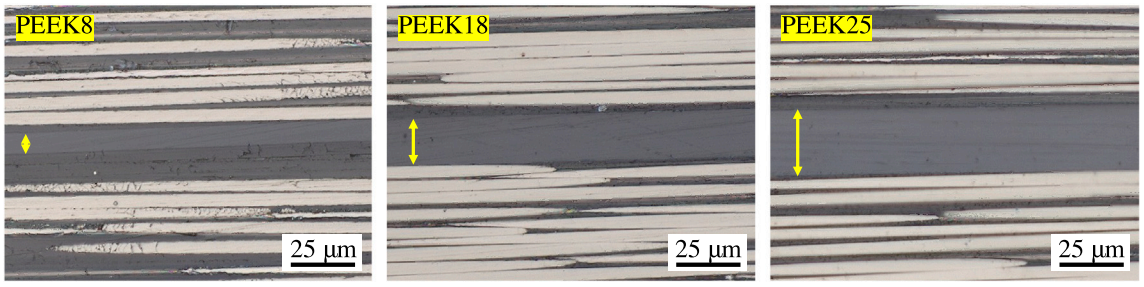

Fig. 2. Side-view images of the interleaved laminates. The yellow colour double head arrows indicate the interlayers.

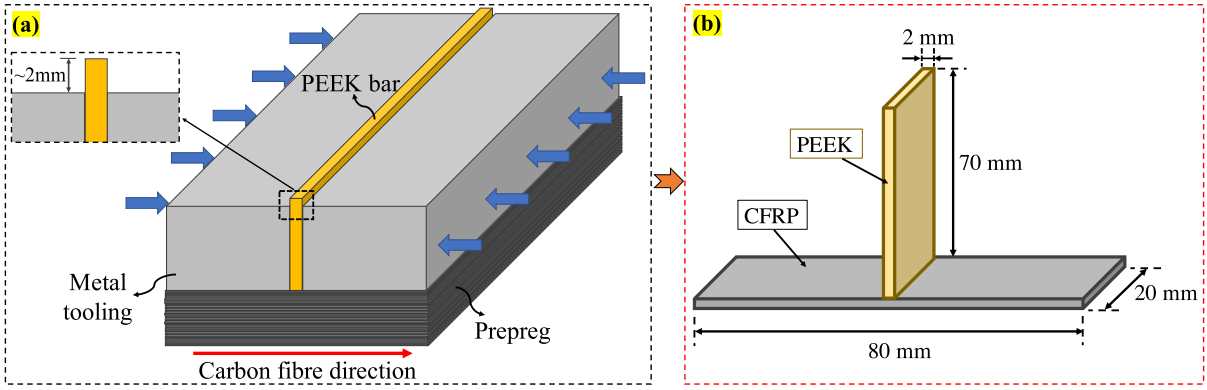

Fig. 3. A schematic of the (a) T-joint layup and (b) T-joint specimens.

different durations. The PEEK bar was then supported by clamping two pieces of steel tools against it using two G-clamps at both ends and the hight of the PEEK bar was 2 mm larger than the steel tools, as shown by Fig. 3 (a). This setup can avoid any bending of the PEEK bar during the following high-pressure curing process, and also ensure a sufficient pressure can be applied onto the PEEK bar and the laminate during the following curing process. The assemble in Fig. 3 (a) was then sealed in a vacuum bag on an Aluminium plate for a 20 min of de-bulking at an under pressure lower than 100 mbar. After the de-bulking, the assemble was placed in the autoclave for curing, with a same curing schedule as the interleaved laminates being applied. The cured joints were then cut into individual specimens according to the dimensions in Fig. 3 (b) for the following tensile test.

2.2. Testing and characterisation

The water contact angles of the PEEK films subject to different durations of UV-treatment were measured using an Attension Theta contact angle meter. A 5 μL water drop was loaded on the surfaces of the PEEK films for the contact angle measurements, that were repeated for five times on different locations of the samples in each case. To measure the failure strength of the T-joint specimens, the PEEK bar was pulled up at a constant displacement of 0.5 mm/min, with the composite substrate being clamped onto the machine. At least three replicable tests were performed for each set of test. The mode-I DCB test and the mode-II ENF test were carried out according to the ASTM-D5528 [28] and ASTM-D7905 [29], respectively. The dimensions and schematics of the DCB and ENT specimens are shown in Fig. 1 (b). A constant displacement rate of 2 mm/min and 0.5 mm/min was used for the DCB and ENF tests, respectively. The crack lengths of the DCB and ENF specimens were measured using a high resolution digital camera during the tests, and then synchronised with the load and displacement measurements based on the start time of the test. An opening load was applied to the DCB and ENF specimens to generate a precrack with a length of about 5 mm from the crack starter, see Fig. 1 (b). Three replicate tests were carried out for each set of DCB and ENF tests. A

modified beam theory method was used to evaluate the mode-I fracture energy, G_{IC} [28]:

$$G_{IC} = \frac{3P\delta}{2b(a+|\Delta|)} \quad (1)$$

where P is the load, δ is the load point displacement, b is specimen width and a is the crack length. The mode-II fracture energy, G_{IIC} was determined using a compliance calibration (CC) method, as described in [29]:

$$G_{IIC} = \frac{3mP_{max}^2 a_{pc}^2}{2b} \quad (2)$$

where P_{max} is the maximum load, a_{pc} is actual crack length used for the ENF test and m is the CC coefficient, that was obtained by carrying the CC tests with a precrack length of 20 mm, 30 mm and 40 mm [29].

The failure surfaces of the PEEK sides of the T-joints and the fracture surfaces of the DCB and ENF specimens were imaged using a VK-X1000 microscope from KEYENCE Corporation and a JSM-7500F scanning electron microscope (SEM) from JOEL. The samples for the SEM analysis were gold sputter coated at a current of 30 mA for 15 s to get a gold layer of approximately 5 nm.

3. Results and discussion

3.1. Failure strength of the T-joints

Fig. 4 presents the results of the water contact angle measurements and the T-joint tensile tests. It should be noted that the values of the T-joint failure strength for a UV-treatment time of 0 min and 0.5 min were not measurable, as the specimens failed prior to the testing due to a low interface adhesion. It was observed that applying the UV-treatment to the PEEK films gradually reduced their surface water contact angles from 84.10° to 30.45° as the treatment time increased from 0 min to 15 mins. No further decrease in the water contact angle was observed as the treatment time increased from 15 mins to 20 mins. During the UV treatment, the high-power UV lights provided sufficient energy to break the C–C/C–H species of the PEEK molecular chain, which was associated with the formation of C–O, C=O and O–C=O species [27,30]. The increased amount of oxygen functional groups on the PEEK surfaces significantly increased the polar component of their surface free energies, that considerably decreased the water contact angle and enhanced the polar-to-polar interaction at the PEEK/epoxy interface. The polar-to-polar interactions typically generate strong Coulomb interactions between permanent dipoles and between permanent and induced dipoles, e.g. hydrogen bonds, and hence, the adhesion between the PEEK films and the epoxy matrix of the laminates had been significantly improved [27,31]. Consequently, the failure strengths of the T-joints steadily increased from zero up to 8.6 MPa as the UV-treatment time increased from 0 min to 15 mins, above where the value dropped to 7.7 MPa for a treatment time of 20 mins, as shown in Fig. 4. The failure strength measurements of the T-joints qualitatively proved an enhanced adhesion at the PEEK/epoxy interface upon the UV-treatment. Based on these results, PEEK films treated by UV lights for a duration of 6 mins and 15 mins were used to interlay the laminates, as they possessed high but different levels of adhesion with the epoxy matrix. Fig. 5 shows the failure surfaces of the PEEK sides of the T-joints subject to a UV-treatment lasting for 0 min, 6 mins and 15 mins. It was obvious that applying the UV-treatment to the PEEK substrates results in extensive carbon fibre peeling-off from the laminate sides of the T-joints, owing to the improved interface adhesion.

3.2. Mode-I fracture behaviour of the laminates

Fig. 6 shows representative load versus displacement curves and corresponding R-curves from the DCB tests of the reference and the interleaved laminates. It was found that interleaving PEEK films resulted in an alteration of the crack growth characteristics from stable

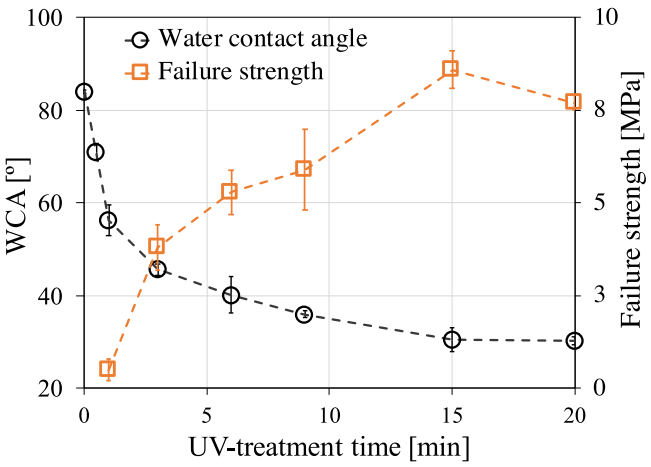

Fig. 4. Water contact angles of the PEEK films and failure strengths of the T-joints versus the duration of the UV-treatment.

propagation for the reference laminate to stick–slip propagation for the interleaved laminates in all the cases, as representatively shown in Fig. 6 (a). During a stick–slip fracture process, the crack propagated forward (or jumped) at the peak points and arrested at the valley points of the load versus displacement curves. In this case, the values of the peak points shall be used for the calculation of the fracture propagation energy [32]. Since the mode-I crack jumped extensively for the interleaved laminates, only a number of values were obtained on the corresponding R-curve in Fig. 6 (b). One can see that the R-curve of the reference laminate was relatively flat, while the values of G_{IC} varied significantly with the crack length for the interleaved laminates due to the unstable crack propagation behaviour.

The mode-I fracture initiation energy (G_{IC}^{ini}) and mode-I fracture propagation energy (G_{IC}^{prop}) of the laminates are summarised in Fig. 7. Clearly, the addition of PEEK film interlayers significantly increased the mode-I fracture toughness of the laminates in all the cases. In particular, a value of 291 J/m^2 and 320 J/m^2 was measured for G_{IC}^{ini} and G_{IC}^{prop}, respectively for the reference laminate. For the laminates interleaved with PEEK(6UV) films, the mode-I fracture toughness steadily increased as the thickness of the PEEK films increased from 8 μm to 25 μm. Interlaying PEEK25(6UV) films into the reference laminate increased G_{IC}^{ini} and G_{IC}^{prop} to 454 J/m^2 and 636 J/m^2, respectively, corresponding to an increase of 56% and 99%, respectively. An improved PEEK film/epoxy adhesion due to applying the UV-treatment for a longer time (15 mins) further improved the toughening performance of the PEEK films. The highest mode-I toughness improvements were obtained by interleaving the PEEK8(15UV) film, that resulted in an increase of 227% and 144% in G_{IC}^{ini} and G_{IC}^{prop}, respectively. Applying a longer time UV-treatment to the PEEK18 and PEEK25 films had also further improved the mode-I fracture toughness of the corresponding laminates. However, the effects were not as prominent as that for the PEEK8 films.

The fracture surfaces of the DCB specimens were analysed to investigate the toughening mechanisms of the interlayers. Noteworthily, the PEEK8 films were separately discussed since they exhibited different toughening mechanisms as the PEEK18 and PEEK25 films. Fig. 8 shows the photographs and microscopy images of the fracture surfaces of the reference and the PEEK8 interleaved laminates. From Figs. 8 (a)–(c), it was obvious that the main fracture mechanisms of the reference laminate were carbon fibre delamination and breakage. Narrow stripes of white colour features (indicated by the black arrows) were observed at the crack onset locations of the laminate interleaved with PEEK8(6UV) film, see Fig. 8 (e). This was caused by the plastic deformation and fracture of the PEEK interlayers during the fracture process, as shown in Fig. 8 (f). A higher PEEK/epoxy adhesion by increasing the UV-treatment duration to 15 mins resulted in significantly higher intensity

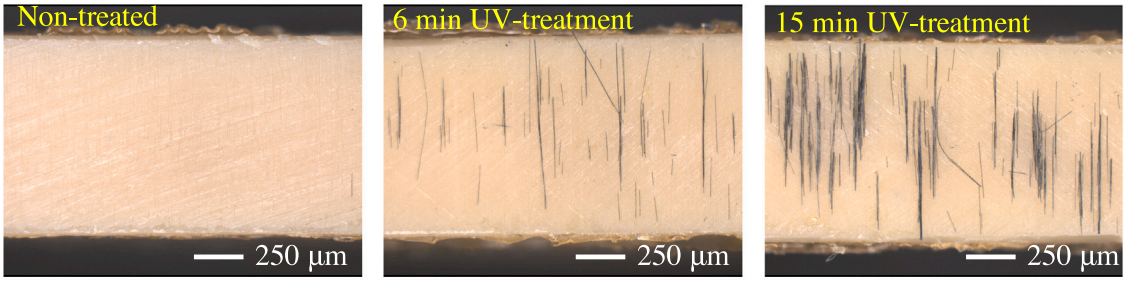

Fig. 5. Failure surfaces of the PEEK sides of the T-joints.

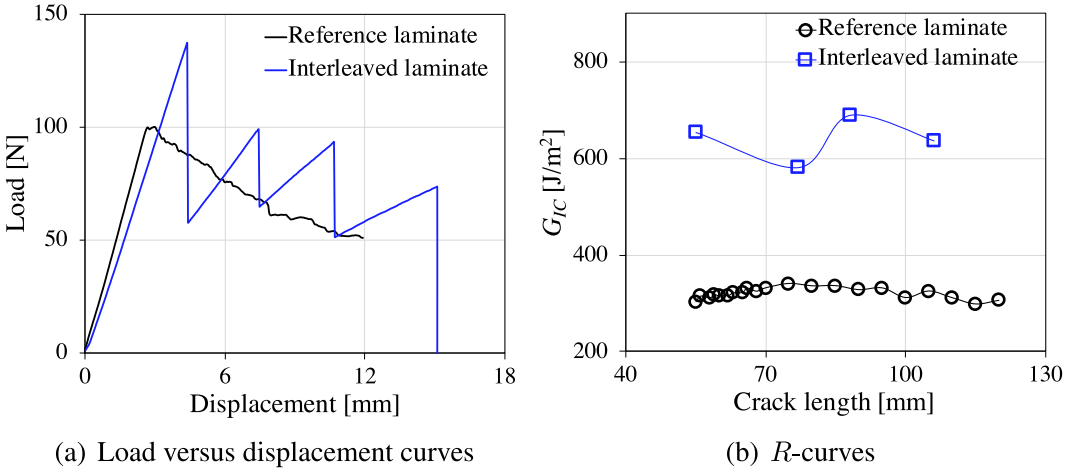

(a) Load versus displacement curves (b) R-curves

Fig. 6. Representative load versus displacement curves and R-curves from the DCB tests of the reference and the interleaved laminates.

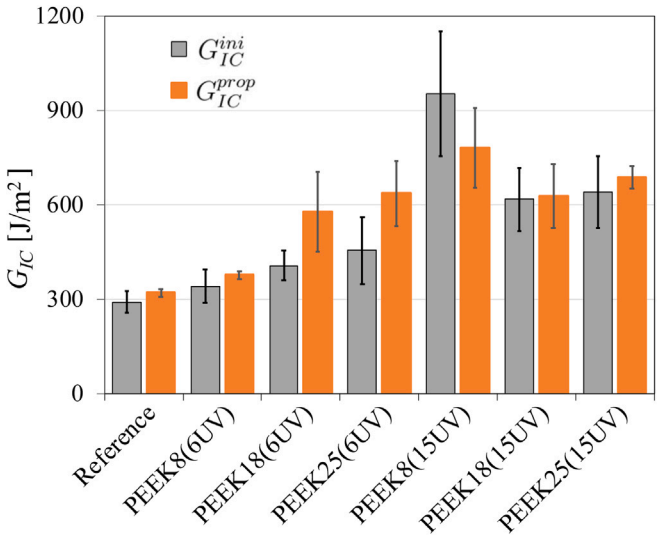

Fig. 7. A summary of the mode-I fracture energies.

of plastic deformation and fracture of the PEEK film during the fracture process, see Figs. 8 (i) and (j). This explained why an outstanding toughening performance was observed for the PEEK8(15UV) film in Fig. 7. Representative photographs of the mode-I fracture surfaces for the laminates interleaved with PEEK18 and PEEK25 films are shown in Fig. 9. Fractured PEEK pieces were observed on both sides of the fracture surfaces for all the displayed laminates, indicating extensive PEEK deformation and fracture during the crack propagation process. By taking a closer look at Fig. 9, it was found that wherever PEEK polymer appeared on one side of the fracture surfaces, black colour regions presented at the same locations on the opposite side for all the laminates interleaved with PEEK18 and PEEK25 films. These observations indicated that the crack took place in a manner that is schematically shown in Fig. 10. Accordingly, significant PEEK film debonding and splitting occurred during the fracture process, that was associated with extensive plastic deformation and fracture of PEEK polymer, as shown by the microscopy images in Fig. 10. These mechanisms contributed to the significant toughness improvements of the laminates. As such, an increased PEEK/epoxy adhesion by increasing the UV-treatment time from 6 mins to 15 mins improved the toughening effectiveness of the PEEK debonding mechanism, and subsequently resulted in a better toughening performance of the PEEK18 and PEEK25 films.

3.3. Mode-II fracture behaviour of the laminates

Representative load versus displacement curves from the ENF tests are shown in Fig. 11. The curves for the reference laminate and the laminates interleaved with PEEK(6UV) films were moved to the right for easy observation. It was observed that interleaving the UV-treated PEEK films significantly increased the failure load of the ENF specimens in all the cases, and the failure load increased with an increasing thickness of the PEEK films. For example, the failure load of the reference specimen shown in Fig. 11 was 1285 N. This value considerably increased to a maximum value of 3546 N for the laminate interleaved with the PEEK25(15UV) films. Additionally, it was found that applying a longer time UV-treatment to the PEEK films resulted in higher failure loads of the ENF specimens. Fig. 12 summarises the mode-II fracture energies (G_{IIC}) of all the laminates obtained from the ENF tests. As expected, significant increases in G_{IIC} of the laminates were observed due to interleaving the PEEK films in all the cases. For both of the UV-treatment durations, a steady increase in G_{IIC} was observed as the

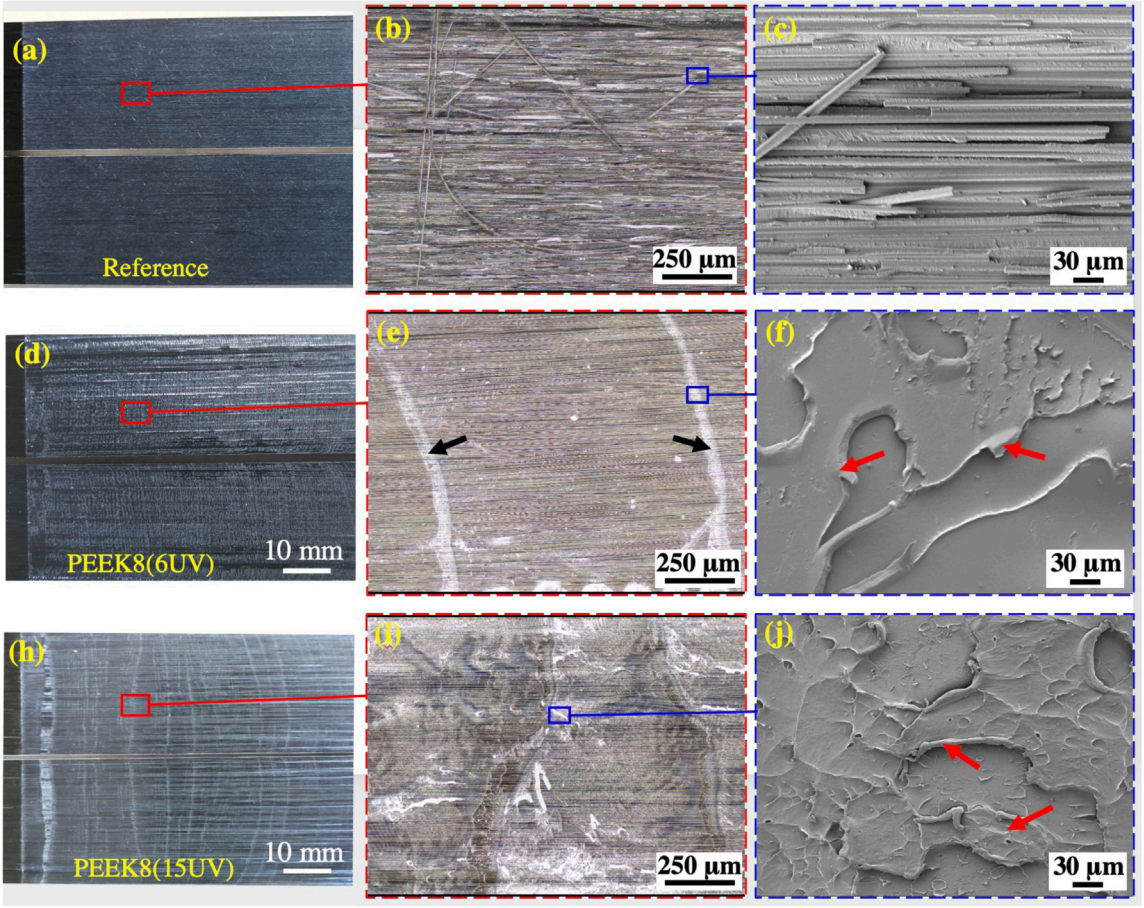

Fig. 8. Photographs and typical microscopy images of the mode-I fracture surfaces of the reference and PEEK8 interleaved laminates. The black arrows in (e) indicate the crack onset locations, while the red colour arrows in (f) and (j) indicate fractured PEEK films.

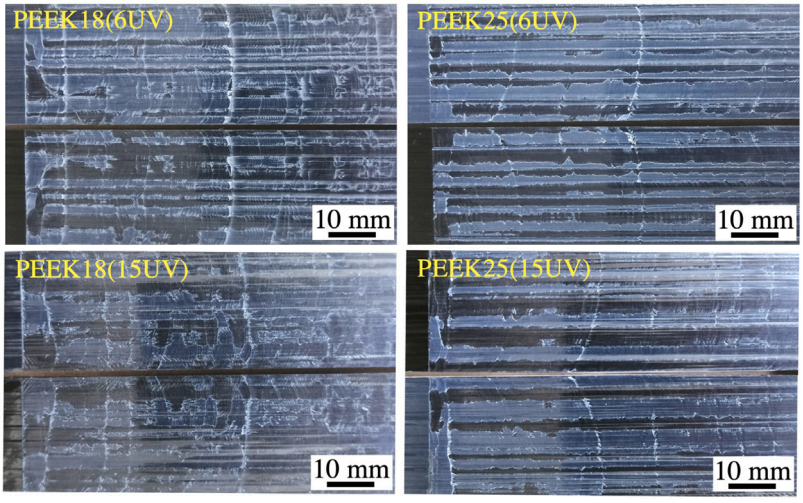

Fig. 9. Photographs of the fracture surfaces of the DCB specimens for the laminates interleaved with PEEK18 and PEEK25 films.

thickness of the PEEK films increased from 8 μm to 25 μm. In particular, G_{IIC} of the non-interleaved laminate was measured to be 1.14 kJ/m^2. Interleaving the PEEK25(6sUV) film into the laminate significantly increased G_{IIC} to 5.60 kJ/m^2, corresponding to an increase of 393%. The use of PEEK25(15UV) film as interlayers further increased the value of to G_{IIC} 6.15 kJ/m^2. This corresponded to an increase of 441% when compared with the value of the reference laminate.

Fig. 13 presents the photographs of the mode-II fracture surfaces of the reference and the interleaved laminates. The yellow dashed lines indicate the fronts of the precracks that were generated by an opening load. The mode-II crack propagation region was referred to as the area on the right side of the precrack front. By comparing the mode-II fracture surfaces of the reference and the interleaved laminates, it was observed that the fracture surfaces of the interleaved laminates were covered extensive white colour features. This indicated obvious

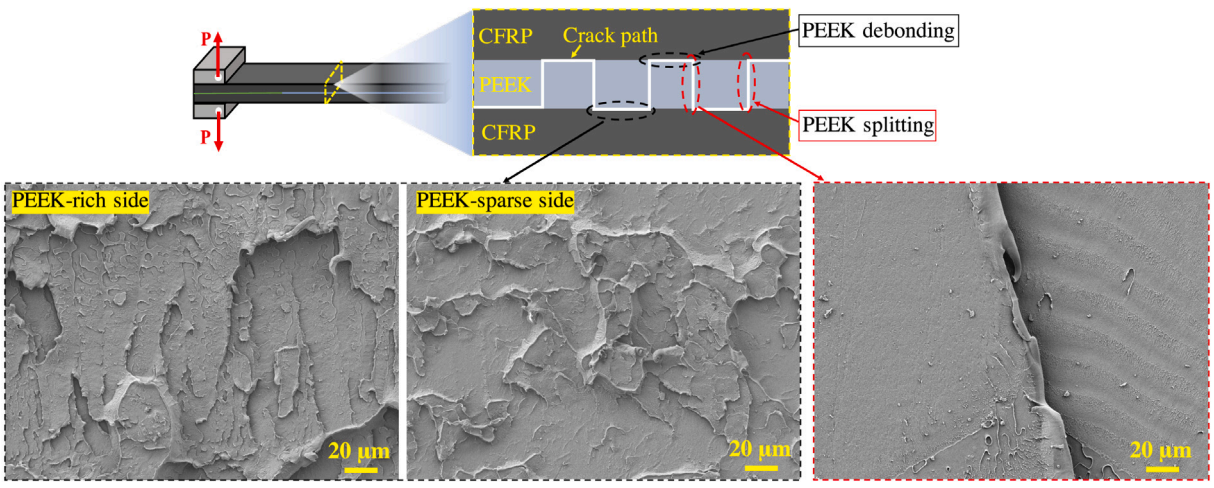

Fig. 10. A schematic for showing the fracture mode of the laminates interleaved with PEEK18 and PEEK25 films, together with typical SEM images of the fracture surfaces.

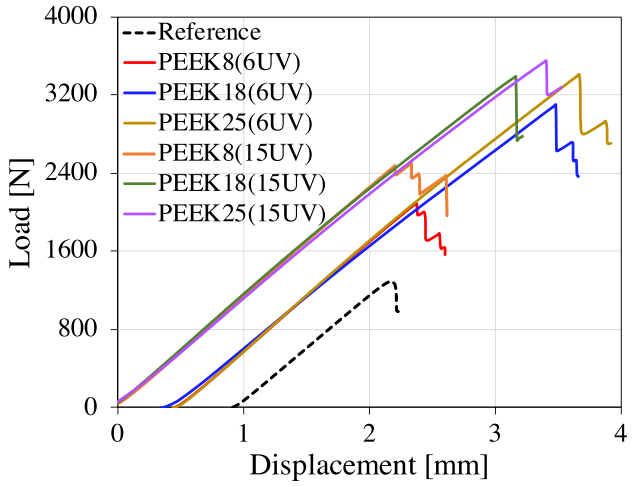

Fig. 11. Representative load versus displacement curves of the ENF tests for the reference and all the interleaved laminates.

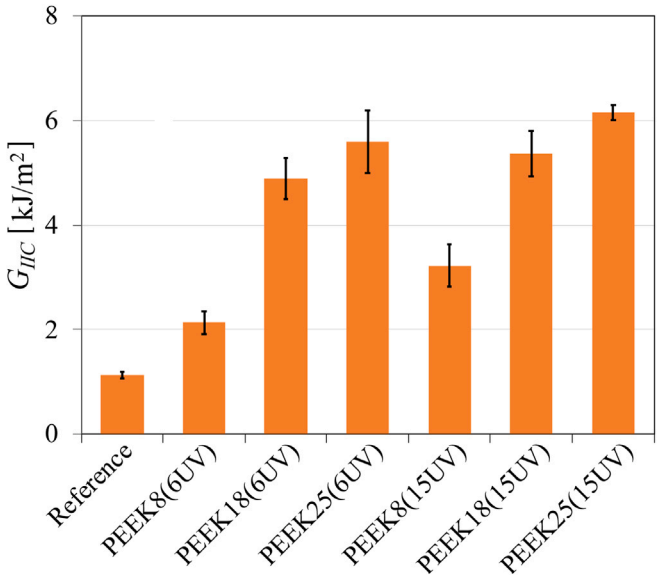

Fig. 12. A summary of the mode-II fracture energies.

damage to the strong and tough PEEK films during the mode-II fracture process of all the interleaved laminates, that resulted in the significant improvements of the mode-II fracture toughness. By observing the fracture surfaces carefully, it was found that the damage of the PEEK interlayers was more intense for the PEEK(15UV) films than the PEEK(6UV) films in all the cases. This explained why PEEK(15UV) film exhibited better toughening performances for the mode-II fracture of the laminates than the PEEK(6UV) films. Noteworthily, the mode-II fracture surfaces appeared differently at different crack lengths in all the cases. This was caused by different fracture mechanisms of the PEEK films, as representatively shown in Fig. 14. Obviously, extensive plastic deformation and damage of the PEEK films in different forms occurred at different stages of the mode-II fracture process. These mechanisms resulted in the remarkable improvements of the mode-II fracture energies of the laminates.

4. Comparison with the state of the art

Table 1 summarises recent achievements of interlayer toughening using various materials in the literature, together with the results of this study. It should be noted that only the maximum increases in the fracture toughness from each literature were included in the table for a comparison purpose. As already discussed in Section 1, significantly different levels of toughening performance were observed for various interlayer materials. Among all the listed state of the art studies, the toughening performance of the PEEK films subject to 15 min UV-treatment (used in this study) exhibited an outstanding toughening performance for both of the mode-I and mode-II fracture modes. Moreover, the toughening performance of interlayers based on PEEK polymer was exceptional for the mode-II fracture, i.e. the levels of mode-II toughness improvements obtained in the current work and in the literature [24] were extraordinary. Noteworthily, the excellent toughening effectiveness obtained in this work was based on a good adhesion at the PEEK/epoxy interface, which was sufficient to cause significant plastic deformation and fracture of the PEEK polymer during the fracture process, as shown by the typical SEM images of the mode-I and mode-II fracture surfaces in Figs. 8, 10 and 14. Moreover, the very small thickness of these PEEK films can essentially avoid the drops of carbon fibre volume fractions due to interlaying, and hence retain the in-plane mechanical properties of the laminates.

5. Conclusions

This study demonstrated a possibility of utilising the exceptional mechanical properties and fracture toughness of PEEK polymers for interlayer toughening of carbon fibre/epoxy laminates. This was achieved

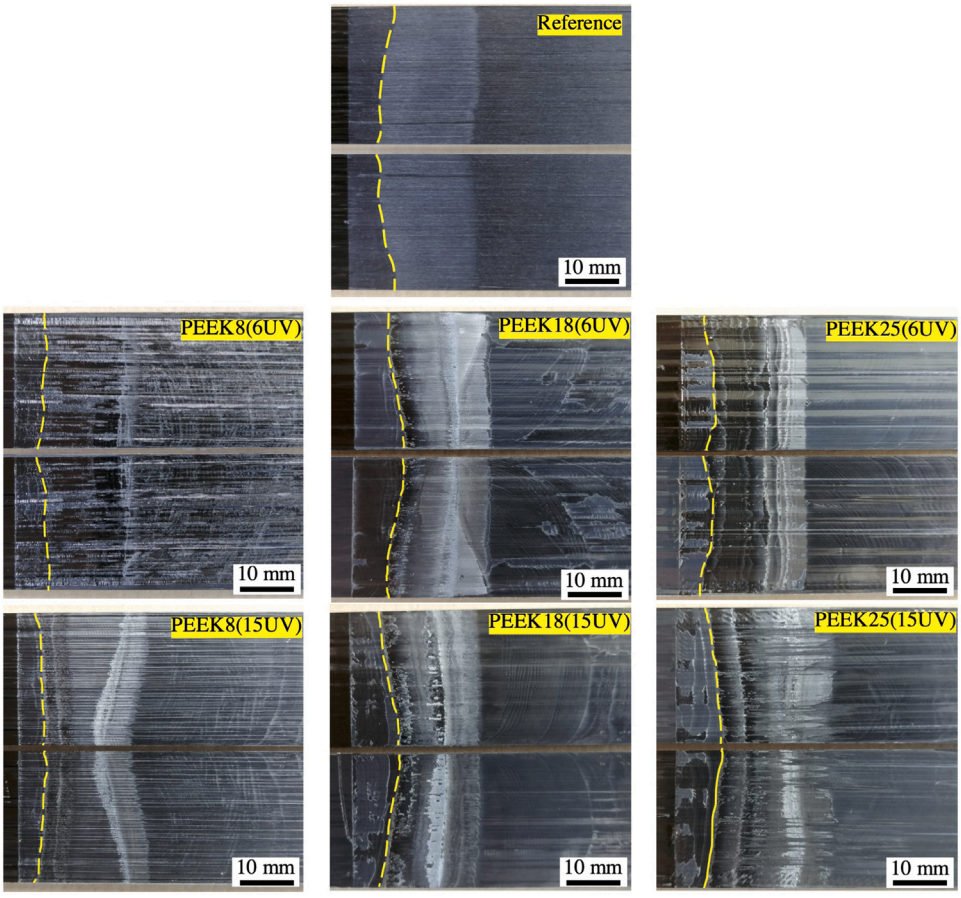

Fig. 13. Photographs of the mode-II fracture surfaces. The yellow dashed lines indicate the fronts of the precracks.

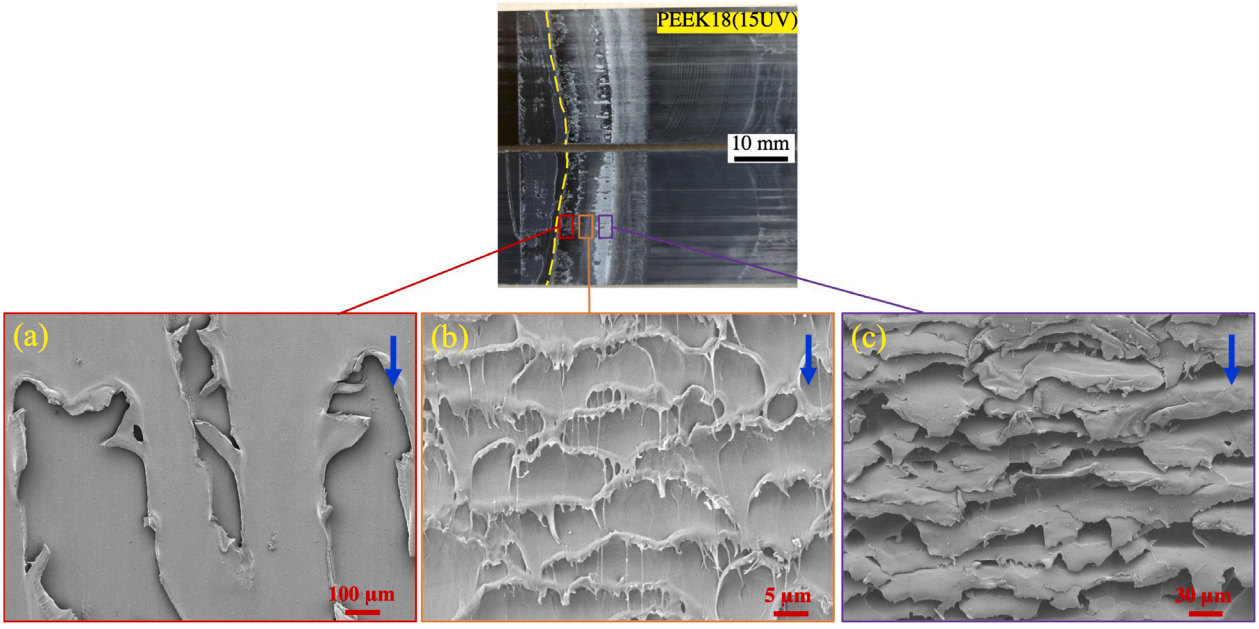

Fig. 14. Different fracture mechanisms of the PEEK films at different stages of the mode-II fracture process of the laminates.

by significantly enhancing the adhesion between the PEEK interlayers and the epoxy matrix upon promoting the surface activities of the PEEK interlayers. In specific, ultra-thin PEEK films with a thickness of 8 μm, 18 μm and 25 μm were used as interlayers of an aerospace grade carbon fibre/epoxy composite, with an attempt to simultaneously enhance the mode-I and mode-II fracture toughness. The surfaces of the PEEK films were treated using a UV-irradiation technique prior to the interlaying. The failure strength measurements of the T-joint specimens between PEEK bars and laminate substrates proved that the adhesion at the PEEK film/epoxy interface can be tailored by varying the durations of

Table 1
Toughening performance of different interlayers for carbon fibre/epoxy composites.

Literature	Interlayer material	Amount of veils	Type of composites	G_{IC} (% increase)	G_{IIC} (% increase)
Carbon nanomaterials					
[33]	CNT veils	30 μm	5H-satin woven	66%(G_{IC}^{prop})	*
[34]	Aligned CNTs	40-55 μm	Unidirectional	0%	>50%
[35]	CNT veils	0.2 g/m^2	Unidirectional	171%(G_{IC}^{ini}); 108%(G_{IC}^{prop})	*
[36]	graphene	*	Unidirectional	41%(G_{IC}^{ini})	69%
[37,38]	hybrid graphene/CNTs	0.2 g/m^2	Unidirectional	102%(G_{IC}^{prop})	154%
Short fibres					
[39]	sCF nowoven	150 μm	Plain woven	99%(G_{IC}^{prop})	109%
[40,41]	sCF nowoven	100 μm	Unidirectional	28%	260%
[42]	sCF nowoven	10 g/m^2	Plain woven	73%(G_{IC}^{prop})	*
[42]	CNTs/sCFs	1.8/10 g/m^2	Plain woven	29%(G_{IC}^{ini}), 125%(G_{IC}^{prop})	*
[43]	CNTs/sCFs	*	Unidirectional	35%(G_{IC}^{prop})	246%
Thermoplastic nowovens					
[44]	PA6,6	40 μm	Unidirectional	56%(G_{IC}^{ini}); 8%(G_{IC}^{prop})	61%
[45]	PA69	18 g/m^2	Unidirectional	25%(G_{IC}^{ini}); -9%(G_{IC}^{prop})	211%
	PA66	18 g/m^2	Unidirectional	4%(G_{IC}^{ini}); -27%(G_{IC}^{prop})	188%
[32,46]	PE	23 g/m^2	Unidirectional	65%(G_{IC}^{ini}); 20%(G_{IC}^{prop})	57%
	PA	21 g/m^2	Unidirectional	−55%(G_{IC}^{ini}); -51%(G_{IC}^{prop})	92%
[9,10]	PET	17 g/m^2	Unidirectional	127%(G_{IC}^{ini}); 173%(G_{IC}^{prop})	181%
	PPS	15 g/m^2	Unidirectional	74%(G_{IC}^{ini}); 216%(G_{IC}^{prop})	187%
	PA	10 g/m^2	Unidirectional	86%(G_{IC}^{ini}); 85%(G_{IC}^{prop})	300%
[47]	PES	28.3 g/m^2	Plain woven	92.7%(G_{IC}^{ini}); 103%(G_{IC}^{prop})	69%
[24]	PEEK	11 g/m^2	Unidirectional	100%(G_{IC}^{ini}); 69%(G_{IC}^{prop})	340%
	PPS	35 g/m^2	Unidirectional	238%(G_{IC}^{ini}); 100%(G_{IC}^{prop})	540%
[26]	CNTs/PPS	0.25/5 g/m^2	Unidirectional	36%(G_{IC}^{ini}); 71%(G_{IC}^{prop})	211%
[48]	CNTs/PET	0.4/8 g/m^2	Unidirectional	56%(G_{IC}^{ini}); 64%(G_{IC}^{prop})	116%
Thermoplastic films					
[17,18]	PI stripes	50 μm	Unidirectional	70%(G_{IC}^{prop})	118%
[20]	structured PEK-C	21 μm	Unidirectional	17%(G_{IC}^{prop})	325%
[19]	PEK-C	10 μm	Unidirectional	91%(G_{IC}^{ini}); 51%(G_{IC}^{prop})	*
[22]	ABS	30,60 μm	Unidirectional	*	no improvement
[49]	Porous PES	97.5 μm	Plain woven	62%(G_{IC}^{prop})	55.1%
This study	PEEK	8 μm	Unidirectional	227%(G_{IC}^{ini}); 144%(G_{IC}^{prop})	183%
	PEEK	18 μm	Unidirectional	227%(G_{IC}^{ini}); 112%(G_{IC}^{prop})	372%
	PEEK	25 μm	Unidirectional	119%(G_{IC}^{ini}); 114%(G_{IC}^{prop})	441%

* sCF: short carbon fibres; sGF: short glass fibres.

the UV-treatment. Consequently, the interlaminar fracture properties of the laminates had been significantly increased upon interleaving the UV-treated PEEK films. In particular, a maximum increase of 227% and 441% was obtained for the mode-I and mode-II fracture energies, respectively by interleaving the PEEK films that were UV-irradiated for 15 mins. A fractography analysis on the fractured specimens revealed significant plastic deformation and fracture of the PEEK interlayers during the fracture process. An overview of the state-of-the-art showed that the toughening effectiveness of the UV-treated PEEK films is superior to the other advanced interlayer materials, owing to the exceptionally strong and tough characteristics of the PEEK polymers. In summary, this experimental study demonstrated a significant potential of interlaying ultra-thin PEEK films on the develop of strong and tough composite laminates, especially for the aerospace applications.

CRediT authorship contribution statement

Dong Quan: Conceptualization, Investigation, Writing – original draft. **Guilong Wang:** Resources, Investigation, Writing – review & editing. **Guoqun Zhao:** Methodology, Writing – review & editing. **René Alderliesten:** Resources, Methodology, Writing – review & editing.

Declaration of competing interest

The authors declare that they have no known competing financial interests or personal relationships that could have appeared to influence the work reported in this paper.

Data availability

Data will be made available on request.

Acknowledgements

The authors would like to acknowledge the financial supports from the key research and development program of Shandong Province, China (Grant No. 2021ZLGX01), the Natural Science Foundation of Shandong Province, China (Grant No.: 2022HWYQ-013), and the National Natural Science Foundation of China (NSFC, Grant No. 51875318).

References

[1] Quan D, Alderliesten R, Dransfeld C, Murphy N, Ivankovic A, Benedictus R. Enhancing the fracture toughness of carbon fibre/epoxy composites by interleaving hybrid meltable/non-meltable thermoplastic veils. Compos Struct 2020;252:112699. http://dx.doi.org/10.1016/j.compstruct.2020.112699.

[2] Gong Y, Chen X, Zou L, Li X, Zhao L, Zhang J, et al. Experimental and numerical investigations on the mode I delamination growth behavior of laminated composites with different z-pin fiber reinforcements. Compos Struct 2022;287:115370. http://dx.doi.org/10.1016/j.compstruct.2022.115370.

[3] Jabbar M, Shaker K, Nawab Y, Umair M. Effect of the stuffer yarns on the mechanical performance of novel 3D woven green composites. Compos Struct 2021;269:114023. http://dx.doi.org/10.1016/j.compstruct.2021.114023.

[4] Quade DJ, Jana SC, Morscher GN, Kanaan M. The effect of thin film adhesives on mode I interlaminar fracture toughness in carbon fiber composites with shape memory alloy inserts. Eng Fract Mech 2019;206:131–46. http://dx.doi.org/10.1016/j.engfracmech.2018.11.040.

[5] He Y, Zhang J, Yao L, Tang J, Che B, Ju S, et al. A multi-layer resin film infusion process to control CNTs distribution and alignment for improving CFRP interlaminar fracture toughness. Compos Struct 2021;260:113510. http://dx.doi.org/10.1016/j.compstruct.2020.113510.

[6] Quan D, Flynn S, Artuso M, Murphy N, Rouge C, Ivankovic A. Interlaminar fracture toughness of CFRPs interleaved with stainless steel fibres. Compos Struct 2019;210:49–56. http://dx.doi.org/10.1016/j.compstruct.2018.11.016.

[7] Wang J, Ma C, Chen G, Dai P. Interlaminar fracture toughness and conductivity of carbon fiber/epoxy resin composite laminate modified by carbon black-loaded polypropylene non-woven fabric interleaves. Compos Struct 2020;234:111649. http://dx.doi.org/10.1016/j.compstruct.2019.111649.

[8] Arnold M, Henne M, Bender K, Drechsler K. The influence of various kinds of PA12 interlayer on the interlaminar toughness of carbon fiber-reinforced epoxy composites. Polym Compos 2015;36(7):1249–57. http://dx.doi.org/10.1002/pc.23029.

[9] Quan D, Bologna F, Scarselli G, Ivankovic A, Murphy N. Mode-II fracture behaviour of aerospace-grade carbon fibre/epoxy composites interleaved with thermoplastic veils. Compos Sci Technol 2020;191:108065. http://dx.doi.org/10.1016/j.compscitech.2020.108065.

[10] Quan D, Bologna F, Scarselli G, Ivankovic A, Murphy N. Interlaminar fracture toughness of aerospace-grade carbon fibre reinforced plastics interleaved with thermoplastic veils. Composites A 2020;128:105642. http://dx.doi.org/10.1016/j.compositesa.2019.105642.

[11] Nash N, Young T, McGrail P, Stanley W. Inclusion of a thermoplastic phase to improve impact and post-impact performances of carbon fibre reinforced thermosetting composites - a review. Mater Des 2015;85:582–97. http://dx.doi.org/10.1016/j.matdes.2015.07.001.

[12] Palazzetti R, Zucchelli A, Gualandi C, Focarete M, Donati L, Minak G, et al. Influence of electrospun nylon 6,6 nanofibrous mats on the interlaminar properties of Gr-epoxy composite laminates. Compos Struct 2012;94(2):571–9. http://dx.doi.org/10.1016/j.compstruct.2011.08.019.

[13] Palazzetti R, Zucchelli A. Electrospun nanofibers as reinforcement for composite laminates materials-A review. Compos Struct 2017;182:711–27. http://dx.doi.org/10.1016/j.compstruct.2017.09.021.

[14] Palazzetti R, Zucchelli A, Trendafilova I. The self-reinforcing effect of Nylon 6,6 nano-fibres on CFRP laminates subjected to low velocity impact. Compos Struct 2013;106:661–71. http://dx.doi.org/10.1016/j.compstruct.2013.07.021.

[15] Beylergil B, Tanoglu M, Aktas E. Enhancement of interlaminar fracture toughness of carbon fiber/epoxy composites using polyamide-6,6 electrospun nanofibers. J Appl Polym Sci 2017;134(35):45244. http://dx.doi.org/10.1002/app.45244.

[16] Cugnoni J, Amacher R, Kohler S, Brunner J, Kramer E, Dransfeld C, et al. Towards aerospace grade thin-ply composites: Effect of ply thickness, fibre, matrix and interlayer toughening on strength and damage tolerance. Compos Sci Technol 2018;168:467–77. http://dx.doi.org/10.1016/j.compscitech.2018.08.037.

[17] Yasaee M, Bond I, Trask R, Greenhalgh E. Mode I interfacial toughening through discontinuous interleaves for damage suppression and control. Composites A 2012;43(1):198–207. http://dx.doi.org/10.1016/j.compositesa.2011.10.009.

[18] Yasaee M, Bond I, Trask R, Greenhalgh E. Mode II interfacial toughening through discontinuous interleaves for damage suppression and control. Composites A 2012;43(1):121–8. http://dx.doi.org/10.1016/j.compositesa.2011.09.026.

[19] Yao J, Zhang T, Niu Y. Effect of curing time on phase morphology and fracture toughness of PEK-C film interleaved carbon fibre/epoxy composite laminates. Compos Struct 2020;248:112550. http://dx.doi.org/10.1016/j.compstruct.2020.112550.

[20] Guo M, Liu L. Structuring the thermoplastic interleaf with lotus-leaf-like structure and its interlaminar toughening for CFRPs. Compos Sci Technol 2019;183:107825. http://dx.doi.org/10.1016/j.compscitech.2019.107825.

[21] Mathew E, Joshi SC, Manikandan P. Enhancement in interply toughness of BMI composites using micro-thin films. J Composites Sci 2021;5(2):49. http://dx.doi.org/10.3390/jcs5020049.

[22] Marino SG, Czel G. Improving the performance of pseudo-ductile hybrid composites by film-interleaving. Composites A 2021;142:106233. http://dx.doi.org/10.1016/j.compositesa.2020.106233.

[23] Quan D, Deegan B, Binsfeld L, Li X, Atkinson J, Ivankovic A, et al. Effect of interlaying UV-irradiated PEEK fibres on the mechanical, impact and fracture response of aerospace-grade carbon fibre/epoxy composites. Composites B 2020;191:107923. http://dx.doi.org/10.1016/j.compositesb.2020.107923.

[24] Ramirez VA, Hogg PJ, Sampson WW. The influence of the nonwoven veil architectures on interlaminar fracture toughness of interleaved composites. Compos Sci Technol 2015;110:103–10. http://dx.doi.org/10.1016/j.compscitech.2015.01.016.

[25] Quan D, Deegan B, Alderliesten R, Dransfeld C, Murphy N, Ivanković A, et al. The influence of interlayer/epoxy adhesion on the mode-I and mode-II fracture response of carbon fibre/epoxy composites interleaved with thermoplastic veils. Mater Des 2020;192:108781. http://dx.doi.org/10.1016/j.matdes.2020.108781.

[26] Quan D, Mischo C, Binsfeld L, Ivankovic A, Murphy N. Fracture behaviour of carbon fibre/epoxy composites interleaved by MWCNT- and graphene nanoplatelet-doped thermoplastic veils. Compos Struct 2020;235:111767. http://dx.doi.org/10.1016/j.compstruct.2019.111767.

[27] Quan D, Alderliesten R, Dransfeld C, Tsakoniatis I, Teixeira De Freitas S, Scarselli G, et al. Significantly enhanced structural integrity of adhesively bonded PPS and PEEK composite joints by rapidly UV-irradiating the substrates. Compos Sci Technol 2020;199:108358. http://dx.doi.org/10.1016/j.compscitech.2020.108358.

[28] ASTM Standard D5528-13(2013). Standard test method for mode I interlaminar fracture toughness of unidirectional fiber-reinforced polymer matrix composites, ASTM international. ASTM standard D5528-13, ASTM; 2013.

[29] ASTM Standard D7905/D7905M-19(2019). Standard test method for Mode II interlaminar fracture toughness of unidirectional fiber-reinforced polymer matrix composites, ASTM international. ASTM standard D7905/D7905M-19, ASTM; 2019.

[30] Quan D, Alderliesten R, Dransfeld C, Tsakoniatis I, Benedictus R. Co-cure joining of epoxy composites with rapidly UV-irradiated PEEK and PPS composites to achieve high structural integrity. Compos Struct 2020;251:112595. http://dx.doi.org/10.1016/j.compstruct.2020.112595.

[31] Quan D, Deegan B, Byrne L, Scarselli G, Ivankovic A, Murphy N. Rapid surface activation of carbon fibre reinforced PEEK and PPS composites by high-power UV-irradiation for the adhesive joining of dissimilar materials. Composites A 2020;137:105976. http://dx.doi.org/10.1016/j.compositesa.2020.105976.

[32] Kuwata M, Hogg P. Interlaminar toughness of interleaved CFRP using non-woven veils: Part 1. Mode-I testing. Composites A 2011;42(10):1551–9. http://dx.doi.org/10.1016/j.compositesa.2011.07.016.

[33] Ou Y, González C, Vilatela JJ. Interlaminar toughening in structural carbon fiber/epoxy composites interleaved with carbon nanotube veils. Composites A 2019;124:105477. http://dx.doi.org/10.1016/j.compositesa.2019.105477.

[34] Nguyen FN, Tun ST, Haro AP, Hirano N, Yoshioka K, Ovalle-Robles R, et al. Interlaminar reinforcement by aligned carbon nanotubes in carbon fiber reinforced polymer composites. In: 19th International conference on composite materials. Montreal, Canada; 2013.

[35] Nistal A, Falzon BG, Hawkins SC, Chitwan R, García-Diego C, Rubio F. Enhancing the fracture toughness of hierarchical composites through amino-functionalised carbon nanotube webs. Composites B 2019;165:537–44. http://dx.doi.org/10.1016/j.compositesb.2019.02.001.

[36] Nasser J, Zhang L, Sodano H. Laser induced graphene interlaminar reinforcement for tough carbon fiber/epoxy composites. Compos Sci Technol 2021;201:108493. http://dx.doi.org/10.1016/j.compscitech.2020.108493.

[37] Liu B, Cao S, Gao N, Cheng L, Liu Y, Zhang Y, et al. Thermosetting CFRP interlaminar toughening with multi-layers graphene and MWCNTs under mode I fracture. Compos Sci Technol 2019;183:107829. http://dx.doi.org/10.1016/j.compscitech.2019.107829.

[38] Liu B, Gao N, Cao S, Ye F, Liu Y, Zhang Y, et al. Interlaminar toughening of unidirectional CFRP with multilayers graphene and MWCNTs for Mode II fracture. Compos Struct 2020;236:111888. http://dx.doi.org/10.1016/j.compstruct.2020.111888.

[39] Xu F, Yang B, Feng L, Huang D, Xia M. Improved interlaminar fracture toughness and electrical conductivity of CFRPs with non-woven carbon tissue interleaves composed of fibers with different lengths. Polymers 2020;12:803. http://dx.doi.org/10.3390/polym12040803.

[40] Lee S-H, Noguchi H, Kim Y-B, Cheong S-K. Effect of interleaved non-woven carbon tissue on interlaminar fracture toughness of laminated composites: Part I- Mode II. J Compos Mater 2002;36(18):2153–68. http://dx.doi.org/10.1177/0021998302036018981.

[41] Lee S-H, Noguchi H, Kim Y-B, Cheong S-K. Effect of interleaved non-woven carbon tissue on interlaminar fracture toughness of laminated composites: Part I-Mode II. J Compos Mater 2002;36(18):2169–81. http://dx.doi.org/10.1106/002199802026980.

[42] Zhou H, Du X, Liu H-Y, Zhou H, Zhang Y, Mai Y-W. Delamination toughening of carbon fiber/epoxy laminates by hierarchical carbon nanotube-short carbon fiber interleaves. Compos Sci Technol 2017;140:46–53. http://dx.doi.org/10.1016/j.compscitech.2016.12.018.

[43] Lee S-H, Kim H, Hang S, Cheong S-K. Interlaminar fracture toughness of composite laminates with CNT-enhanced nonwoven carbon tissue interleave. Compos Sci Technol 2012;73:1–8. http://dx.doi.org/10.1016/j.compscitech.2012.09.011.

[44] Brugo T, Palazzetti R. The effect of thickness of Nylon 6,6 nanofibrous mat on Modes I-II fracture mechanics of UD and woven composite laminates. Compos Struct 2016;154:172–8. http://dx.doi.org/10.1016/j.compstruct.2016.07.034.

[45] Daelemans L, van der Heijden S, Baere ID, Rahier H, Paepegem WV, Clerck KD. Nanofibre bridging as a toughening mechanism in carbon/epoxy composite laminates interleaved with electrospun polyamide nanofibrous veils. Compos Sci Technol 2015;117:244–56. http://dx.doi.org/10.1016/j.compscitech.2015.06.021.

[46] Kuwata M, Hogg P. Interlaminar toughness of interleaved CFRP using non-woven veils: Part 2. Mode-II testing. Composites A 2011;42(10):1560–70. http://dx.doi.org/10.1016/j.compositesa.2011.07.017.

[47] Cheng C, Chen Z, Huang Z, Zhang C, Tusiime R, Zhou J, et al. Simultaneously improving mode I and mode II fracture toughness of the carbon fiber/epoxy composite laminates via interleaved with uniformly aligned PES fiber webs. Composites A 2020;129:105696. http://dx.doi.org/10.1016/j.compositesa.2019.105696.

[48] Quan D, Mischo C, Li X, Scarselli G, Ivankovic A, Murphy N. Improving the electrical conductivity and fracture toughness of carbon fibre/epoxy composites by interleaving MWCNT-doped thermoplastic veils. Compos Sci Technol 2019;182:107775. http://dx.doi.org/10.1016/j.compscitech.2019.107775.

[49] Cheng C, Zhang C, Zhou J, Jiang M, Sun Z, Zhou S, et al. Improving the interlaminar toughness of the carbon fiber/epoxy composites via interleaved with polyethersulfone porous films. Compos Sci Technol 2019;183:107827. http://dx.doi.org/10.1016/j.compscitech.2019.107827.